ReLo is a simple and quick colocalization assay to identify and characterize direct protein-protein interactions

Harpreet Kaur Salgania[1], Jutta Metz[1], Mandy Jeske[1]*

[1] Heidelberg University Biochemistry Center (BZH), Im Neuenheimer Feld 328, 69120 Heidelberg, Germany

*Correspondence: jeske@bzh.uni-heidelberg.de

ABSTRACT

The characterization of protein-protein interactions (PPIs) is fundamental for understanding biochemical processes. Many methods have been established to identify and study direct PPIs; however, the screening and investigation of PPIs involving large or poorly soluble proteins remain challenging. As a result, we developed ReLo, a simple, rapid, and versatile cell culture-based method for detecting and investigating interactions in a cellular context. Importantly, our data strongly suggest that with ReLo specifically direct binary PPIs are detected. By applying additional bridging experiments ReLo can also be used to determine the binding topology of subunits within multiprotein complexes. Moreover, ReLo has the potential to identify protein domains that mediate complex formation, screen for interfering point mutations, study interactions that depend on conformation or protein arginine methylation, and it is sensitive to drugs that mediate or interfere with an interaction. Taken together, ReLo is a simple and quick alternative for the study of PPIs particularly when established methods fail.

INTRODUCTION

The identification and characterization of protein-protein interactions (PPIs) are a routine laboratory practice and lay the foundation for understanding biological processes. PPIs can be identified through various established, mass spectrometry-coupled screening methods, including coimmunoprecipitation (co-IP), tandem affinity purification, and proximity-dependent labeling approaches, such as BioID or APEX [1–6]. Thus, a list of interacting protein candidates is obtained, and these candidates are usually ranked according to their abundance in eluate fractions. Determining which of these candidates are truly direct binding partners requires subsequent validation experiments, often involving *in vitro* methods, such as GST pull-down assays, which depend upon the availability of purified proteins. If the proteins are poorly soluble and cannot be obtained through recombinant protein expression or if expertise in recombinant protein expression and purification methods is lacking, PPIs can be validated using cell-based assays.

Yeast two-hybrid (Y2H) and protein complementation assays (PCA) are well-established techniques in which an interaction results in the reconstitution and subsequent detection of a split reporter protein, such as a transcription factor, ubiquitin, an enzyme, or a fluorescent protein [7–12]. However, standard Y2H and PCA assays are not particularly suitable for the analysis of potentially unstable proteins, as they are barely expressed or rapidly degraded in a cell, resulting in unreliable, mostly false-negative results [7,10]. Therefore, to obtain conclusive findings, negative results require additional assessment of the protein expression levels, which complicates the process, particularly when probing many PPIs.

Cell-based PPI methods that are better suited for testing interactions involving potentially unstable proteins are based on fluorescent protein tagging and colocalization readouts and thus allow the simultaneous monitoring of both PPIs and

27 protein expression levels via fluorescence microscopy. The readout of these
28 colocalization assays is usually the translocation of one protein upon its association
29 with a second distinctly localized protein (e.g., localization to a membrane, the nucleus,
30 or granules). 'Cytoskeleton-based assay for protein-protein interaction' (CAPPI),
31 'membrane recruitment assay' (MeRA), and 'knocksideways in plants' (KSP) are
32 translocation assays developed for use with plant cells [13–15]. 'Nuclear translocation
33 assay' (NTA), 'emerging circle of interactive proteins at specific endosomes'
34 (ECLIPSE), and 'protein interactions from imaging of complexes after translocation'
35 (PICT) are assays that require the addition of a compound (e.g., rapamycin) to monitor
36 the translocation upon a PPI [16–18]. Other translocation assays are based on
37 oligomerization/aggregation readouts [19–21] and may thus not be suitable for studying
38 interactions with proteins that form granules on their own within a cell. Importantly,
39 none of the described translocation assays have been assessed based on their ability
40 to distinguish direct binary interaction from those where the two proteins tested are
41 eventually bridged by cell-endogenous proteins.

42 We developed a simple and fast translocation PPI assay named ReLo for use
43 with an animal cell culture. This assay is based on the relocalization of a protein upon
44 its interaction with a second membrane-anchored protein. We applied ReLo to many
45 large proteins, most of which harbor long disordered regions and are known to be
46 insoluble after recombinant protein expression experiments. Using this set of proteins,
47 we demonstrate that ReLo can be employed to identify and characterize PPIs.
48 Importantly, using two structurally well-characterized multidomain protein complexes,
49 we show that only direct interactions are detected using ReLo, a prerequisite for the
50 analysis of previously unknown protein complexes through *in vitro* and structural
51 biology methods. Furthermore, ReLo is responsive to drug treatment, which enables
52 the study of drug-induced interactions and the screening of small PPI inhibitors. In

53 summary, ReLo is a simple, rapid and versatile tool that enables a thorough initial
54 description of direct PPI networks.
55
56 **RESULTS**
57 **ReLo: a simple and robust cell culture-based PPI assay**
58 As a preparation for the ReLo assay, two proteins of interest were fused to a red
59 fluorescent protein (mCherry) and a green fluorescent protein (EGPF, mEGFP).
60 Importantly, one of the constructs carried an additional fusion to a membrane-
61 anchoring protein domain, which led to distinct subcellular membrane localization of
62 the fusion protein. Upon interaction, the second protein is expected to colocalize with
63 the anchored protein to the membrane and it would thereby relocalize with respect to
64 its original location (**Fig. 1a)**. Thus, we refer to the assay as the 'relocalization PPI
65 assay', abbreviated 'ReLo'.
66 ReLo is based on a simple methodology in which cells are seeded onto 4-well
67 chambered coverslips and cotransfected with the desired combination of plasmids.
68 After 48 h, the protein localization is analyzed by live-cell confocal fluorescence
69 microscopy (**Fig. 1a)**. We used S2R+ cells, which were derived from semiadherent
70 Schneider's-line-2 (S2) cells, which in turn have been established from late *Drosophila*
71 embryos [22,23]. Compared with S2 cells, S2R+ cells show greater adherence to dishes,
72 and thus they do not require coated dishes for their adhesion prior to live-cell
73 microscopy. All ReLo plasmids carry an in-frame blunt end restriction site, allowing the
74 application of a simple, fast, and straightforward cloning procedure (see Methods
75 section).
76 For the anchoring of cytoplasmic proteins of interest to a membrane, we
77 selected the pleckstrin homology (PH) domain of rat phospholipase Cδ_1 (PLCδ_1), which
78 specifically recognizes phosphatidylinositol 4,5-bisphosphate [24,25] and thus directs the

79 fusion construct to the plasma membrane of a cell (**Fig. 1a)**. In the ReLo assay, the
80 membrane localization was independent of whether the PH domain was fused to the
81 N- or C-terminus of a protein (**Supplementary Fig. 1a)**. Unfortunately, nuclear proteins
82 fused to the PH domain were only inefficiently retained within the cytoplasm and barely
83 localized to the plasma membrane (**Supplementary Fig. 1c)**. Hence, the testing of
84 PPIs to a nuclear protein may result in false-negative outcomes if the interaction
85 partner resides in the cytoplasm. Therefore, we tested alternative membrane-
86 anchoring domains to assess their ability to retain nuclear proteins within the
87 cytoplasm. Hence, we selected the minimembrane protein subunit 4 of the yeast
88 oligosaccharyltransferase complex (OST4), which was previously used as N-terminal
89 fusion protein to localize a nuclear protein to the endoplasmic reticulum (ER) [26,27]
90 (**Supplementary Fig. 1d**). Because the plasma membrane localization of the PH
91 domain distinguishes from a ubiquitous cytoplasmic localization better than the ER
92 localization of OST4, we prefer using the PH domain in ReLo whenever possible.
93
94 **PPI mapping and mutational analysis**
95 As a proof of concept for interaction studies with ReLo, we tested a previously
96 characterized protein complex consisting of the extended LOTUS (eLOTUS) domain
97 of Oskar (Oskar 139-240) and the C-terminal RecA-like domain (CTD) of the ATP-
98 dependent DEAD-box RNA helicase Vasa (Vasa-CTD, Vasa 463-661) [28] (**Fig. 1b)**.
99 Only the short isoform of Oskar (Short Oskar, aa 139-606) interacts with Vasa [29], and
100 therefore, only Short Oskar and its domains were used in the following experiments
101 (**Fig. 1b)**. In our setup, the eLOTUS domain of Oskar was fused to PH-mCherry and
102 localized to the plasma membrane. Vasa-CTD was fused to EGFP and localized
103 ubiquitously within the cytoplasm and nucleus. When coexpressed with PH-mCherry-
104 eLOTUS but not with PH-mCherry alone, EGFP-Vasa-CTD relocalized to the plasma

105 membrane (**Fig. 1c)**. The unstructured region of Vasa (Vasa 1-200) and the N-terminal
106 RecA-like domain (Vasa 200-463) did not interact with the Oskar-eLOTUS domain,
107 and similarly, neither the unstructured region of Oskar (Oskar 241-387) nor its OSK
108 domain (Oskar 388-606) interacted with Vasa-CTD (**Fig. 1c)**. Surface point mutations
109 that had been previously shown to interfere with the Vasa-Oskar interaction [28] were
110 also found to be inhibitory in the ReLo assay (**Fig. 1d**). Together, these data confirmed
111 the specific interaction between Vasa-CTD and Oskar-eLOTUS and demonstrated that
112 ReLo can be applied to map PPIs and to identify mutations that interfere with PPIs.
113 Oskar-eLOTUS and Vasa-CTD form a transient complex characterized by a
114 dissociation constant (K_D) of ~10 μM, and although this complex has been crystallized,
115 it is not sufficiently stable to be detected by size-exclusion chromatography [28,30,31].
116 Nevertheless, the relocalization upon the interaction between Oskar-eLOTUS and
117 Vasa-CTD was clearly detectable in the ReLo assay: in a total of three independent
118 replicates, the relocalization of Vasa-CTD toward the plasma membrane was observed
119 in 91 of 94 (i.e., 97%) cotransfected cells with both red and green fluorescent signals
120 (**Supplementary Fig. 2**). These data indicate that relocalization is a highly frequent
121 event and that the assay is well suited for studying low-affinity complexes. Most other
122 interactions tested revealed relocalization in 100% of the cotransfected cells (see
123 below; **Supplementary Fig. 3**).
124
125 **Conformation-dependent interactions**
126 Previous data have suggested that the Oskar-Vasa interaction depends on the
127 conformation of Vasa [28]. We aimed to test the interaction between Oskar and different
128 Vasa conformations in a full-length protein context. However, in contrast to the
129 eLOTUS domain of Oskar, full-length Short Oskar did not localize to the cytoplasm but
130 exclusively localized to the nucleus in S2R+ cells (**Supplementary Fig. 1b)** [28].

131 Therefore, we made use of the OST4-mCherry-Oskar construct, which localized to
132 membranous structures within the cytoplasm (**Supplementary Fig. 1d and Fig. 1e**).
133 Upon coexpression, wild-type Vasa relocalized and colocalized with OST4-Oskar at
134 the ER (**Fig. 1e**), confirming the interaction between Vasa and Oskar in the ReLo
135 assay. Also using the OST4 anchor, the interaction mapped to the Oskar-eLOTUS
136 domain and the Vasa-CTD **(Supplementary Fig. 1e**) and the known Vasa interface
137 mutant (F504E) was unable to bind to Oskar (**Fig. 1e**), which is consistent with the
138 data obtained using the PH domain (**Fig. 1c, 1d**).

139 The cores of Vasa and other ATP-dependent DEAD-box RNA helicases are
140 composed of two RecA-like domains, which display different orientations relative to
141 each other depending on the presence of bound ATP and RNA [32]. In a substrate-
142 unbound form, the helicase core adopts an open conformation and closes upon
143 substrate binding (**Fig. 2a)**. To assess the conformation-dependent Vasa interaction
144 with the ReLo assay, we used Vasa variants with well-characterized point mutations in
145 the ATP-binding pocket that stabilize either the open conformation (K295N; Vasa-
146 open) or the closed conformation (E400Q; Vasa-closed) [33–35]. When testing the
147 interaction of OST4-anchored Oskar with the Vasa mutants using the ReLo assay, we
148 observed an interaction with Vasa-open but not Vasa-closed (**Fig. 2b)**, which revealed
149 that Oskar prefers to bind to the open conformation of Vasa. These outcomes were
150 consistent with our previous observations [28] and demonstrated that the ReLo assay
151 allows the study of PPIs that are dependent on the specific conformation of an
152 interaction partner.

153

154 **Protein arginine methylation-dependent interactions**

155 Protein interactions may depend on posttranslational modifications, such as protein
156 arginine methylation. The symmetric dimethylated arginine (sDMA) modification is

157 catalyzed by a subset of protein arginine methyltransferases (PRMTs) [36], and sDMA
158 methylation activity has been previously reported in S2 cells [37]. To test whether the
159 ReLo assay is suitable for investigating interactions involving sDMA modifications in
160 S2R+ cells, we tested the previously characterized strictly sDMA-dependent
161 interaction between the PIWI protein Aubergine (Aub) and Tudor [38,39] (**Fig. 2c)**. Using
162 ReLo, we indeed observed an Aub-Tudor interaction (**Fig. 2d**). Aub carries four sDMAs
163 within its RG-rich N-terminus (R11, R13, R15, and R17), which are specifically
164 recognized and bound by extended Tudor (eTud) domains of Tudor [38–41]. The
165 substitution of these four arginine residues with lysine residues (Aub R->K) rendered
166 Aub unmodifiable by PRMT5 [41] and abolished the Aub-Tudor interaction (**Fig. 2d**).
167 Together, these data demonstrated that the S2R+ cells exhibited sufficient sDMA
168 activity to effectively modify proteins expressed after transient transfection of the cells.
169 We conclude that ReLo is suitable for the study of PPIs that depend on PRMT5-
170 catalyzed sDMA modification.
171
172 **Effect of small molecules on PPIs**
173 We subsequently tested whether the ReLo assay can be used to study PPIs that are
174 induced by the addition of small molecules to the cell culture medium. To this end, we
175 tested the previously characterized rapamycin-dependent interaction between human
176 FK506-binding protein 12 (FKBP12) and the FKBP12-rapamycin-binding domain
177 (FRB) of human mTOR [42]. In the absence of rapamycin, using the dimethyl sulfoxide
178 (DMSO)-containing control medium, FKBP12 and FRB did not interact in the ReLo
179 assay but did interact in the presence of 100 nM rapamycin in the cell culture medium
180 (**Fig. 2e**).
181 Furthermore, we tested whether the ReLo assay can be used to inhibit PPIs
182 through drug treatment. We opted to interfere with the interaction between human p53

183 and the human ortholog of mouse double minute 2 (MDM2) using the known
184 peptidomimetic inhibitor nutlin-3 [43]. In the ReLo assay, we used only the N-terminal
185 domains of p53 and MDM2, which were sufficient to mediate the p53-MDM2 interaction
186 [44]. Indeed, although an interaction between p53 1-50 and MDM2 1-118 was detected
187 in the DMSO control experiment, this interaction was not observed when the cells were
188 incubated with 5 μM nutlin-3 (**Fig. 2f**).
189 Together, these data suggest that the ReLo assay can be used to study
190 interactions involving non-*Drosophila* proteins and to screen drugs based on their
191 ability to either enable or inhibit a specific PPI.
192
193 **ReLo reveals direct binary interactions**
194 Thus far, we have tested known direct interactions between proteins that are not
195 endogenously expressed in S2R+ cells. PPIs detected with the ReLo assay may not
196 necessarily involve direct contact. Instead, PPIs may also result from indirect contacts
197 caused by incorporation of the coexpressed pair of proteins into cell-endogenous
198 protein complexes and subsequent indirect bridging of this pair through one or more
199 common interaction partners. To understand the extent to which direct or indirect
200 associations underlie a relocalization event observed with ReLo, we assessed
201 interactions between individual subunits of the CCR4-NOT complex, which is
202 endogenous to S2R+ cells. The CCR4-NOT complex is an essential eukaryotic
203 deadenylase comprising six subunits that form the core with an architecture that is
204 well-characterized at the molecular and structural levels [45,46]. In this complex, NOT1,
205 which has a size of 281 kDa in *Drosophila,* acts as the scaffolding subunit for the
206 assembly of all other subunits. Specifically, the CAF1-CCR4 heterodimer and CAF40
207 bind to the central region of NOT1, and the NOT2-NOT3 subcomplex associates with
208 the C-terminal region of NOT1 (**Fig. 3a)**. Using ReLo, we performed a systematic

209 pairwise screen in which each subunit was tested against all other subunits of the
210 *Drosophila* CCR4-NOT core complex (**Fig. 3b and Supplementary Fig. 4a)**. In S2R+
211 cells, NOT1 and NOT3 localized exclusively to the cytoplasm, whereas NOT2, CAF1,
212 CAF40 and CCR4 localized to both the cyto- and the nucleoplasm (**Supplementary**
213 **Fig. 4b)**. Remarkably, we observed interactions only between proteins that had
214 previously been shown to exhibit direct associations but not between indirectly linked
215 combinations: NOT1 bound specifically to CAF1, CAF40, NOT2, and NOT3, while
216 CAF1 bound to CCR4, and NOT2 bound to NOT3 (**Fig. 3b, c, Supplementary Fig.**
217 **4a, b)**. We also tested the interactions to CAF1 using the OST4 membrane anchor and
218 observed results similar to those obtained using the PH anchor (**Supplementary Fig.**
219 **4c)**. Together, these data suggest that the incorporation of two tagged CCR4-NOT
220 complex subunits into one endogenous complex is insignificant, and thus direct but not
221 indirect interactions between the two proteins tested are observed with the ReLo
222 assay.

223 Although the subunits of the endogenous CCR4-NOT complex show moderate
224 to high expression levels in S2R+ cells [47] (**Supplementary Fig. 5a)**, we aimed to
225 challenge the ReLo assay by testing PPI between subunits of a cytoplasmic complex
226 that is even more abundant in S2R+ cells. We chose the seven-subunit Arp2/3
227 complex, which is known to initiate actin polymerization in eukaryotes [48], and of which
228 several subunits are among the most highly expressed cytoskeletal genes [47,49]
229 (**Supplementary Fig. 5a)**. In S2R+ cells, the Arp2/3 subunits Arp3, Arpc1, and Arpc4
230 are expressed about two- to four-fold higher as compared to NOT3, which is the most
231 abundant subunit of the CCR4-NOT complex (**Supplementary Fig. 5a)**. Compared to
232 the CCR4-NOT complex, binary PPIs within the Arp2/3 complex are less well
233 characterized, and we concluded which subunit is directly or indirectly bound to
234 another subunit based on the crystal structure of the bovine Arp2/3 complex [50]

235 (**Supplementary Fig. 5b, c)**. The crystal structure points to six direct pairwise
236 contacts. Using ReLo assays, we detected two PPIs, namely the Arpc2-Arpc4 and the
237 Arpc4-Arpc5 interaction (**Supplementary Fig. 5c, d**). The other four contacts, which
238 we did not observe with ReLo, were also not detected in an earlier pairwise study of
239 the human Arp2/3 complex using Y2H assays [51]. Importantly, we did not detect any
240 false-positive interaction using the ReLo assay. These data suggest that even if a
241 complex is highly abundant in a cell, the detection of a PPI between two protein
242 candidates in the ReLo assays is direct rather than indirectly mediated by incorporation
243 into the same endogenous complex. Nevertheless, we cannot exclude that
244 occasionally, indirect interactions are detected through a naturally expressed bridging
245 protein.

246 Finally, we compared the ReLo assay to the split-ubiquitin yeast two-hybrid
247 assay [27,52], which we have previously used successfully to map the interaction between
248 Short Oskar and Vasa [30]. When we assessed the pairwise interactions between the
249 six CCR4-NOT complex core subunits using Y2H, we observed mostly false negative
250 and false positive results; the only conclusive interaction that we detected was between
251 NOT2 and NOT3 (**Supplementary Fig. 6**). This observation is in stark contrast to our
252 data obtained using ReLo assays. As both Y2H and ReLo worked well to map the
253 Oskar-Vasa interaction, together the data suggest that the applicability of Y2H for
254 testing interactions is case/project dependent. ReLo could be expected to be more
255 reliable than Y2H for testing large proteins from higher eukaryotes, although a larger
256 scale study would be required to fully test this.

257

258 **Topological description of multisubunit complexes**

259 As has been described for S2 cells [53], we usually observed a very high cotransfection
260 efficiency of the S2R+ cells when performing ReLo experiments. Therefore, we tested

261 whether the bridging of CCR4-NOT subunits that do not directly interact is observable
262 when one or two common binding partners are added to the mixture. Specifically, S2R+
263 cells were cotransfected with three or four plasmids: one plasmid expressing the PH-
264 mCherry fusion construct, one plasmid expressing the mEGFP fusion construct, and
265 one or two plasmids expressing nonfluorescent bridging factors (**Fig. 3d**). Indeed,
266 NOT3 failed to interact with CAF1 or CAF40 in the presence of the control plasmid but
267 interacted when NOT1 was provided in addition (**Fig. 3e, f**). We also tested the bridging
268 of the NOT3-CCR4 interaction, which requires not only NOT1 but also the CAF1
269 subunit. The NOT3-CCR4 interaction was not observed if NOT1 alone was
270 coexpressed but was observed when both NOT1 and CAF1 were coexpressed (**Fig.**
271 **3g**). Similar results were obtained from the testing of indirect interactions with CAF40
272 (**Supplementary Fig. 4d**). Together, these data show that bridging experiments with
273 ReLo can be used to reconstitute the binding topology of multisubunit complexes such
274 as the CCR4-NOT complex.
275
276 **Assessment of PPIs between the CCR4-NOT complex and mRNA repressor**
277 **proteins**
278 The CCR4-NOT complex can be recruited specifically to mRNAs through adapter
279 RNA-binding proteins, which leads to accelerated deadenylation and eventually
280 degradation and/or translational repression of the targeted mRNA. We then assessed
281 PPIs between some of these repressor proteins and the six core subunits of the CCR4-
282 NOT complex using ReLo (**Fig. 4a)**. Co-IP experiments combined with structural
283 analysis previously revealed the specific subunit(s) of the CCR4-NOT complex through
284 which adapter proteins recruit the complex to a specific mRNA. For example,
285 *Drosophila* Bag-of-marbles (Bam) has been shown to bind specifically to CAF40 [54].
286 We confirmed this finding with ReLo: Bam bound to CAF40 but not to any other CCR4-

287 NOT complex subunit (**Fig. 4b and Supplementary Fig. 7a)**. A point mutation in Bam
288 (M24E; Bam MUT), which is known to interfere with CAF40 binding [54], also abolished
289 CAF40 binding in the ReLo assay (**Fig. 4b)**. Likewise, a mutation at the CAF40 surface
290 (V186E; CAF40 MUT), which was shown to prevent Bam binding [54], abolished the
291 interaction with Bam in the ReLo assay (**Fig. 4b)**.[55]

292 *Drosophila* Roquin has been demonstrated to bind to *Drosophila* CAF40. It also
293 binds to the so-called CAF40 module composed of CAF40 and the CAF40-binding
294 region of NOT1 and to the NOT1/2/3 module composed of the C-terminal domains of
295 the NOT1, NOT2, and NOT3 subunits of human CCR4-NOT complex [55]. Of the
296 subunits tested in the ReLo assay, we detected clear binding of Roquin to *Drosophila*
297 CAF40, NOT1, and NOT3 but not to NOT2 (**Fig. 4c and Supplementary Fig. 7b)**,
298 essentially confirming the previous data. In addition, we detected a previously unknown
299 interaction between Roquin and CCR4 (**Fig. 4c**).

300 *Drosophila* Nanos was shown to bind to the NOT1/2/3 module of the human
301 CCR4-NOT complex in GST pull-down experiments, but does not bind to any of these
302 domains individually [56]. With ReLo, we detected the interaction of Nanos with
303 *Drosophila* NOT1 but not with NOT2 or NOT3, which suggests that the NOT1
304 interaction might be predominant (**Fig. 4d and Supplementary Fig. 7c)**. In addition,
305 we detected Nanos binding to the CAF40 subunit (**Fig. 4d)**, an interaction that has not
306 previously been reported.

307 Encouraged by these mostly validating data, we tested the interaction of the
308 CCR4-NOT complex with less well characterized potential adaptor proteins.
309 *Drosophila* meiosis regulator and mRNA stability factor 1 (MARF1) is an oocyte-
310 specific protein that recruits the CCR4-NOT complex to target mRNAs and thereby
311 controls meiosis [57]. *Drosophila* Smaug recruits the CCR4-NOT complex to *nanos* and
312 other mRNAs to regulate posterior patterning and nuclear divisions of the early embryo

313 [58–62]. Whether MARF1 or Smaug directly associate with the CCR4-NOT complex was
314 unknown. Using ReLo, we found that Smaug interacted with the NOT3 subunit [63], and
315 that MARF1 bound to the NOT1 subunit (**Fig. 4e and Supplementary Fig. 7d**), which
316 suggests that Smaug and MARF1 are indeed direct recruiters of the CCR4-NOT
317 complex.

318 *Drosophila* Cup and its orthologous protein 4E-T are translation repressor
319 proteins that act through their interactions with the eukaryotic translation initiation
320 factor 4E (eIF4E) and the DEAD-box RNA helicase Me31B/DDX6 [64–68]. Both the
321 human 4E-T - Me31B and the *Drosophila* Cup-eIF4E complex are structurally
322 characterized [69,70] and we detected both interactions using ReLo assays (**Fig. 4f, left**
323 **panels**). As demonstrated through co-IP experiments, Cup also interacts with the
324 CAF1, CCR4, NOT1, NOT2, and NOT3 subunits of the CCR4-NOT complex [71]. We
325 did not detect Cup binding to any subunit of the CCR4-NOT core complex using ReLo
326 assays (**Supplementary Fig. 7e**), which suggests that if Cup directly recruits the
327 CCR4-NOT complex, then it probably involves weak and multivalent interactions. Cup
328 also reportedly binds the repressors Nanos and Bruno [65,72,73], and with the ReLo assay
329 we confirmed both interactions (**Fig. 4f, right panels**). Consistent with a recent report
330 [74], we also observed that Bruno binds directly to Nanos (**Fig. 4g**). We then asked if
331 Bruno and Nanos bind to Cup as a complex. However, when coexpressed with Cup,
332 Bruno and Nanos did not interact (**Fig. 4g**), which suggests that Bruno and Nanos
333 compete for binding to the same region of Cup. Bruno has thus far not been shown to
334 establish direct contact with the CCR4-NOT complex, and we did not detect Bruno
335 binding to any of the core CCR4-NOT complex subunits (**Supplementary Fig. 7f**).

336 In summary, the assessment of PPIs using ReLo involving a wide selection of
337 repressor proteins, confirmed many previously described interactions and revealed

338 new interactions. Thus, ReLo is a powerful method for identifying novel PPIs in a
339 candidate approach.
340
341 **Combining ReLo assays with structural prediction**
342 Lastly, we aimed to obtain some molecular insight into one of the newly identified
343 interactions. We tested the structural prediction of the Nanos-CAF40 complex using
344 AlphaFold2-multimer-v3 and obtained a high-confidence model as indicated by the
345 predicted aligned error (PAE) plot (**Fig. 4h, Supplementary Fig. 8a**) [75–77]. The
346 predicted structure is composed of full-length CAF40 and a short α-helix spanning
347 residues 140 to 160 of Nanos, which is bound to the same site of CAF40 that was
348 shown to accommodate the Bam or Roquin α-helical peptide [54,55] (**Supplementary**
349 **Fig. 8b**). The CAF40 point mutation that prevented Bam binding (**Fig. 4b**), also
350 abolished the interaction with Nanos (**Fig. 4i**). Likewise, deletion of the CAF40-binding
351 α-helix from Nanos (Nanos Δ140-160) prevented the interaction with CAF40 (**Fig. 4i**).
352 These data are consistent with the predicted structural model of the Nanos-CAF40
353 complex. Taken together, our exemplary analysis suggests that the combination of
354 ReLo assays with structural modeling can lead to fast molecular insight into protein
355 complexes.
356
357 **DISCUSSION**
358 The detection and characterization of PPIs are crucial for uncovering regulatory
359 mechanisms that underlie cellular processes. Here, we described ReLo, a rapid
360 procedure for identifying and investigating pairwise as well as multisubunit PPIs. We
361 provided strong evidence showing that pairwise PPIs identified with ReLo are based
362 on direct contacts. Thus, PPI partners newly identified using ReLo are highly promising
363 candidates for use in subsequent studies using *in vitro* assays and experimental

364 structural biology methods. Alternatively, PPI mapping data obtained from ReLo
365 experiments may be used to guide subsequent modeling experiments using
366 AlphaFold2-Multimer to obtain structural information on complexes [75,76]. A thus
367 predicted protein–protein interface may then rapidly be validated through mutational
368 analysis using ReLo, and the mutations that specifically interfere with a PPI may finally
369 be tested *in vivo* without the need for purifying a protein or experimentally determining
370 a structure of a protein complex.

371 We refrained from quantifying the relocalization events observed with ReLo
372 through image processing tools to assess or compare PPIs. Although only qualitative,
373 the results obtained were typically clear. For example, in control experiments, we never
374 observed relocalization, and in experiments in which proteins interacted, most or all
375 cells showed relocalization (**Supplementary Figs. 2 and 3**). Furthermore, the
376 implementation of a relocalization score as a quantified readout of an interaction may
377 have easily led to the false assumption that the score represents a measure of binding
378 affinity between proteins. Such false assumptions are also an issue with Y2H dot
379 assays, which appear to but do not provide quantitative data. The degree of
380 relocalization identified with the ReLo assay or yeast cell growth in a Y2H assay not
381 only reflects the binding affinity of the protein complex but also relies on the protein
382 expression levels, protein stability, subcellular localization, and other factors. With this
383 thought in mind, we prefer to consider ReLo a qualitative PPI method, the strength of
384 which lies in its speed and versatility.

385 ReLo is easy to perform in every laboratory equipped with cell culture
386 technology and with access to a confocal fluorescence microscope. In contrast to
387 standard Y2H or PCA assays, the expression levels of the proteins tested in a ReLo
388 assay are directly monitored during microscopy, which facilitates data interpretation.
389 The *Drosophila* S2R+ cell line used for our ReLo tests requires very simple handling.

390 Similar to S2 cells, S2R+ cells grow at ambient temperature, do not need an incubator
391 with CO_2, and can be passaged without the need for coated dishes nor the scraping or
392 trypsinization of cells [53]. Using S2R+ cells, we successfully investigated not only
393 *Drosophila* PPIs but also human PPIs. However, when a cell line derived from an
394 alternative organism is needed for a ReLo assay, only the PH or OST4 membrane
395 anchors need to be inserted into expression vectors compatible with the desired cell
396 line.

397 With ReLo assays, we investigated PPIs involving NOT1 and Tudor, two large
398 proteins comprising 281 kDa (2505 aa) and 285 kDa (2515 aa), respectively. Thus, the
399 detection of PPIs using the ReLo assay appears to be successful regardless of the
400 length of the protein of interest, which, in our experience, is a big advantage over Y2H
401 methods. Similar to any other cell-based PPI assay, attention is needed when working
402 with toxic proteins. To reduce toxicity, we recommend testing the splitting of the toxic
403 protein into its domains or, when possible, testing protein variants with mutated active
404 sites.

405 PPIs are highly relevant as putative therapeutic targets for the development of
406 new treatments [78,79]. In ReLo, complex formation is reversible, and we demonstrated
407 that ReLo is a tool for testing the effect of small molecules on PPIs. Due to its simple
408 setup, ReLo might be easily adjusted to a high-throughput approach using automated
409 imaging, which allows for large drug screening experiments. In a setup in which a
410 single specific PPI is subjected to a drug screening experiment, it might be
411 advantageous to express the two protein partners from one plasmid to ensure
412 equimolar protein expression within a cell, which may facilitate data interpretation.

413 Taken together, our data show that investigations with ReLo are rapid, simple,
414 and reliable. We recommend using ReLo as an initial tool to screen and characterize
415 PPIs, particularly in cases in which Y2H or more complicated approaches fail.

416 Subsequently, ReLo can be complemented with biochemical, structural, or genetic
417 approaches to further characterize or ultimately validate the biological relevance of a
418 given PPI.
419

420 **ACKNOWLEDGMENTS**

421 We thank Elmar Wahle, Julien Bethune, Bernd Bukau, and Ivana Vonkova for DNA
422 constructs and Aurelio Telemann for the S2R+ cell line. We are grateful to Christian
423 Bleischwitz, Eva Boberlin, Jana Kubíková, Katharina Müller, Rebecca Reinig, Gabrielė
424 Ubartaitė, and Xiaohan Zhao for technical assistance provided with some experiments.
425 We thank the Nikon Imaging Center at the University of Heidelberg for access to
426 microscopes. We gratefully acknowledge the data storage service SDS@hd supported
427 by the Ministry of Science, Research and the Arts Baden-Württemberg (MWK) and the
428 German Research Foundation (DFG) through the grants INST 35/1314-1 FUGG and
429 INST 35/1503-1 FUGG. We thank Peter Becker, Hüseyin Besir, Julien Béthune, and
430 Doris Höglinger for their insightful comments on the manuscript. This work was funded
431 by the Emmy-Noether Program of the German Research Foundation (DFG; JE-827/1-
432 1).
433

434 **METHODS**

435 **Plasmid backbone construction**

436 pAc5.1-EGFP and pAc5.1-mCherry were described previously [28]. pAc5.1-mEGFP
437 encodes the monomeric A206K EGFP variant and was generated by site-directed
438 mutagenesis of pAc5.1-EGFP. The pAc5.1-λN-HA vector [80] was used to create
439 nonfluorescent constructs. The *Saccharomyces cerevisiae* OST4 sequence was
440 amplified from a pDHB1 vector [27] and inserted into the KpnI site of pAc5.1-mCherry to
441 yield pAc5.1-OST4-mCherry. For cloning into the pAc5.1-EGFP, pAc5.1-mEGFP,

442 pAc5.1-mCherry, pAc5.1-λN-HA, and pAc5.1-OST4-mCherry vectors, sequences of
443 interest were inserted into the blunt-end EcoRV site. The rat PLCδ_1-PH sequence was
444 amplified from the pETM11-His6-PH-Sumo3-sfGFP vector [81] and inserted into the KpnI
445 site of pAc5.1-mCherry and pAc5.1-mEGFP to obtain pAc5.1-PH-mCherry and
446 pAc5.1-PH-mEGFP, respectively. Alternatively, the PH sequence was inserted into the
447 EcoRV site of pAc5.1-mCherry to obtain the pAc5.1-mCherry-PH vector. For all PH-
448 containing vectors, a new unique in-frame FspAI blunt end site was introduced 3' or 5'
449 with respect to the fluorescent protein sequences and was used to insert the sequence
450 of interest.
451
452 **Cloning**
453 Ligation reactions were assembled in a 10 µl reaction containing T4 DNA ligase
454 (Thermo Scientific), 50 ng of vector DNA, and a 5- to 20-fold molar excess of DNA
455 inserts and were incubated for 1 to 2 h at room temperature. DNA inserts were
456 generated by PCR amplification. To prevent re-ligation, the reaction was supplemented
457 with 0.25 µl of the blunt end restriction enzyme that was also used for linearization of
458 the respective vector, except when this site was present in the insert sequence.
459 Positive clones were screened by colony PCR using one primer that binds to the vector
460 and a second that binds to the insert. All constructs were verified by sequencing.
461 Detailed information on all DNA constructs used in this study is listed in
462 **Supplementary Table 1**.
463
464 **Cell culture**
465 S2R+ cells were cultured at 25°C in Schneider's *Drosophila* medium + (L)-glutamine
466 (Thermo Scientific) supplemented with 10% fetal bovine serum (Sigma) and 1 x
467 Gibco™ Antibiotic-Antimycotic (Thermo Scientific). Cells were seeded in six-well

468 glass-bottom plates (Cellvis; earlier experiments) or four-well polymer μ-slides (Ibidi;
469 later experiments) and cotransfected using jetOPTIMUS (Polyplus Transfection)
470 according to the instruction manual. Specifically, 600 μl of cells with a density of
471 $1x10^6$ cells/ml were seeded per well in a four-well slide and 61 μl of transfection
472 reagent mixture was added. This mixture contained 1 μl of transfection reagent and
473 600 ng of DNA in total for cotransfecting two (300 ng DNA each), three (200 ng each),
474 or four (150 ng each) plasmids diluted in jetOPTIMUS buffer. After 48 h of incubation
475 at 25°C, images of live cells were taken with a 60x or 100x oil objective and a Nikon
476 TE2000 laser scanning, a Nikon Ti-E spinning disc confocal, or a Nikon Eclipse Ti2
477 laser scanning fluorescence microscope and processed with Fiji software [82]. Changing
478 the amount of DNA or transfection reagent during the transfection did not change the
479 protein expression levels in the cells. However, reducing the total DNA amount to
480 150 ng and/or the transfection reagent to 0.5 μl significantly reduced the transfection
481 efficiency.
482
483 **Drug treatment**
484
485 Rapamycin and nutlin-3 (both from MedChemExpress) were dissolved in DMSO to
486 obtain stock concentrations of 10.9 mM and 10 mM, respectively, and they were diluted
487 with SF-4 Baculo express medium (BioConcept) to generate working concentrations
488 of 100 nM and 5 μM, respectively. S2R+ cells were grown in SF-4 medium and
489 cotransfected with desired plasmids using FuGENE® HD transfection reagent
490 (Promega). Specifically, cells were seeded as described above and 26 μl of
491 transfection reagent mixture was added. This mixture contained 1 μl of transfection
492 reagent and 400 ng of DNA (i.e., 200 ng DNA each for cotransfecting two plasmids)
493 diluted in SF-4 Baculo express medium. Twenty-four hours after transfection, the cells

494 were treated with the drug by replacing the medium with drug-containing medium. Cells
495 were imaged after 24 h of incubation with the drug or DMSO control medium at 25°C.
496

497 **AUTHOR CONTRIBUTIONS**

498 H.K.S. and J.M. acquired, analyzed, and interpreted the data. M.J. conceived and
499 supervised the project, acquired, analyzed, and interpreted the data, and wrote the
500 manuscript with input from all authors.
501

502 **COMPETING INTEREST**

503 The authors declare no competing interests.
504

505 **DATA AVAILABILITY STATEMENT**

506 The authors declare that all relevant data supporting the findings of this study are
507 available within the article and its supplementary information files.
508

509 **MAIN FIGURES**
510

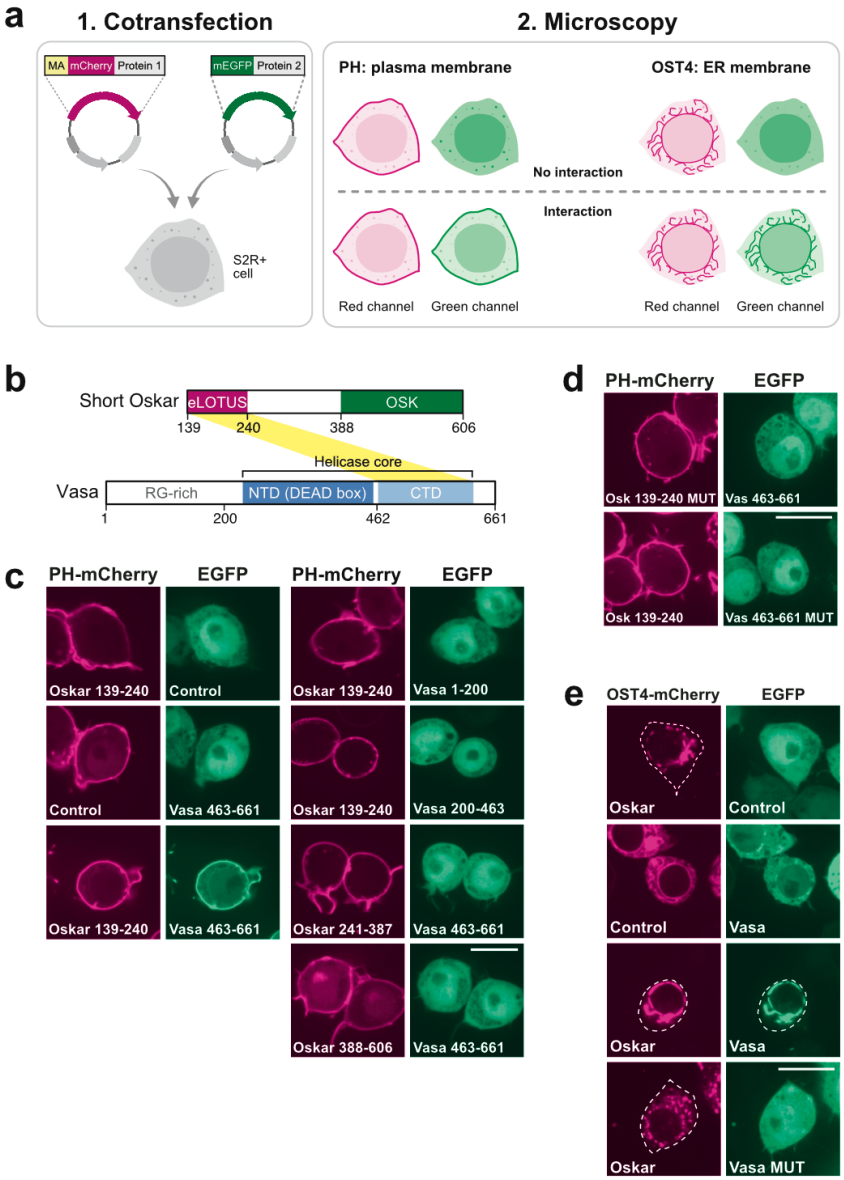

511
512 **Fig. 1. ReLo assay and its use in PPI mapping and mutational analysis.**
513 **a** Plasmids encoding fluorescently tagged proteins 1 and 2 are cotransfected into S2R+
514 cells. Protein 1 carries an additional fusion to a membrane anchoring (MA) domain,
515 i.e., PH or OST4. After 48 h, protein localization is analyzed by confocal fluorescence
516 microscopy. If protein 2 interacts with protein 1, protein 2 is relocalized to the plasma
517 membrane (PH domain) or ER (OST4). **b** Domain organization of *Drosophila* Oskar
518 and Vasa proteins. Oskar is expressed in two isoforms, and Short Oskar lacks amino
519 acids 1-138. The eLOTUS domain of Oskar was previously shown to interact with the
520 C-terminal domain (CTD) of Vasa (yellow stripe), and the crystal structure of the
521 complex has been resolved [28,30]. **c** Vasa 463-661, but not Vasa 1-200 or 200-463,
522 interacted with the Oskar eLOTUS domain. Vasa 463-661 did not interact with Oskar
523 241-396 or Oskar 398-606. **d** Oskar A162E/L228E and Vasa F504E point mutations
524 (MUT) interfered with the Oskar-Vasa interaction. **e** OST4-mCherry Oskar localized to
525 the ER (top panel), and Vasa fully relocalized with Oskar to the ER (bottom panel),
526 while Vasa MUT did not. In the "Control" experiments the respective construct was
527 coexpressed with the vector indicated at the top of the panel lacking an insert. The
528 scale bar is 10 µm.

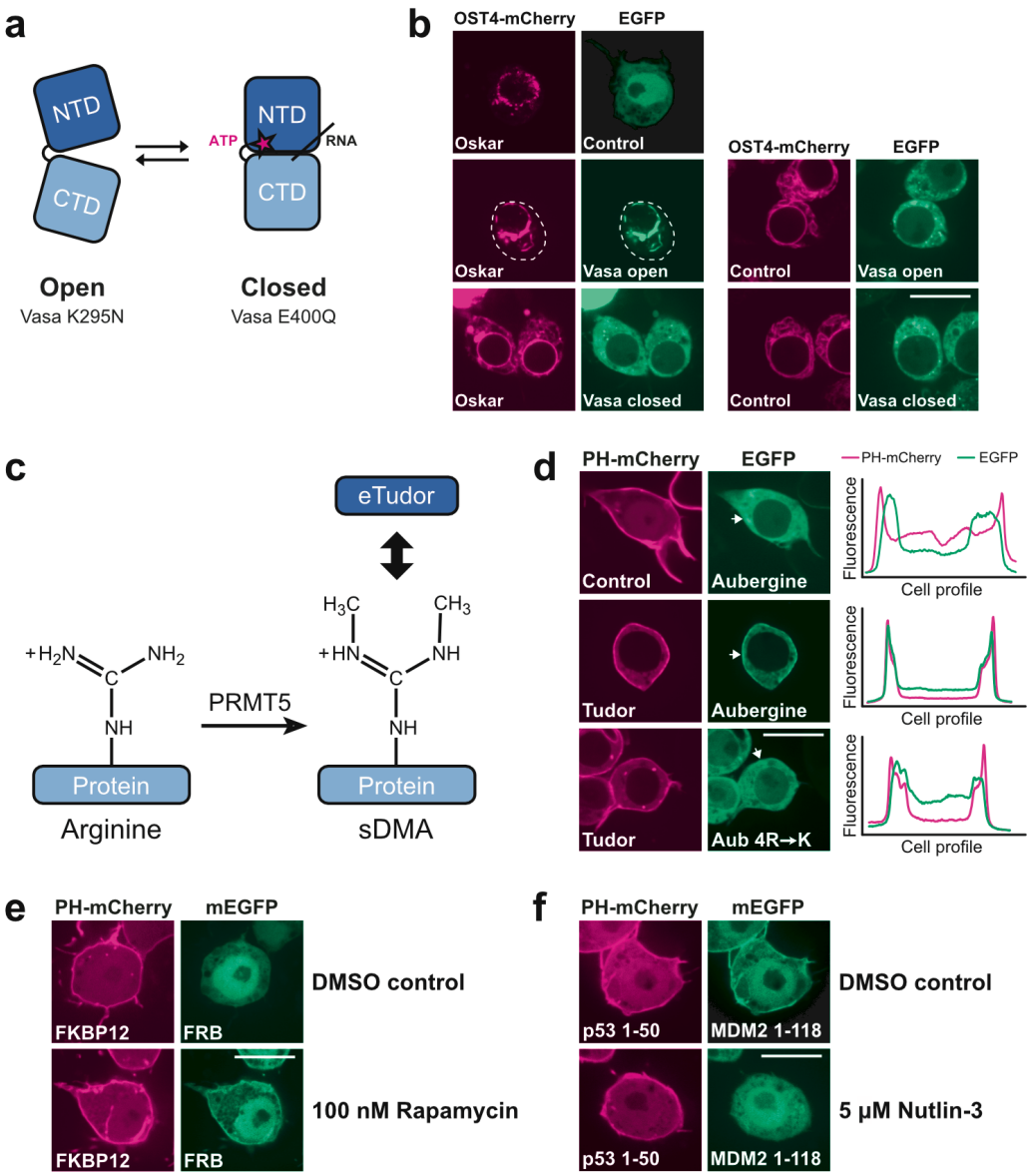

Fig. 2. PPI studies using ReLo with respect to conformation, posttranslational modification and drug sensitivity.
a Pictorial representation of Vasa N- and C-terminal RecA-like domains (NTD and CTD, respectively) in the open and closed conformations. Vasa-open and Vasa-closed carry the K295N or E400Q mutations, respectively. **b** EGFP-Vasa-open, but not EGFP-Vasa-closed, interacted with OST4-mCherry-Oskar. The white dotted lines indicate cell boundaries. **c** Symmetric dimethyl arginine (sDMA) modifications can be catalyzed by PRMT5 and recognized by eTud domains. **d** Wild-type Aub interacted with Tudor, whereas Aub carrying nonmethylatable 4R->K point mutations (R11K/R13K/R15K/R17K) did not. The profiles indicate the measured fluorescence distribution across the cell along a line indicated by the white arrows (shown for the green channel only). Red and green fluorescence signals are independent and displayed relatively. **e** Rapamycin induced an interaction between human FKBP12 and FRB. The control contained 0.0009% dimethyl sulfoxide (DMSO). **f** The interaction between p53 1-50 and MDM2 1-118 was inhibited by nutlin-3 treatment. The control contained 0.05% DMSO. In the "Control" experiments the respective construct was coexpressed with the vector indicated at the top of the panel lacking an insert. The scale bar is 10 μm.

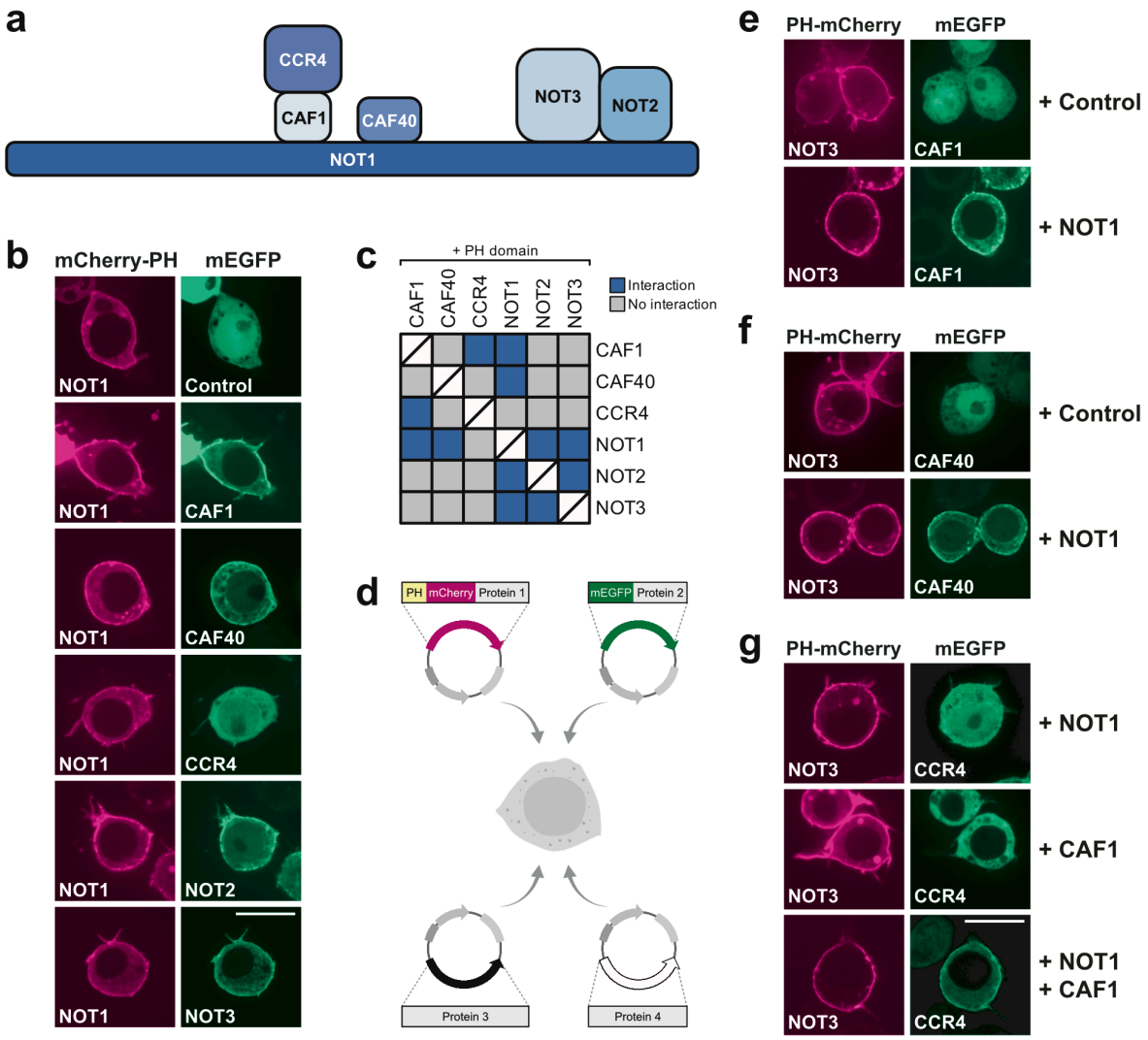

Fig. 3. ReLo identifies direct PPIs.
a Subunit organization of the *Drosophila* CCR4-NOT core complex. **b** NOT1-mCherry-PH recruited CAF1, CAF40, NOT2, and NOT3 but not CCR4 to the plasma membrane. See **Supplementary Fig. 3a** for the PPI analysis of the other CCR4-NOT complex subunits. **c** Summary of the results from a pairwise screen of CCR4-NOT complex core subunits using ReLo. The blue color indicates an interaction, and the gray color indicates no interaction. **d** Schematic showing the ReLo assay involving coexpression of four different protein constructs. **e** NOT3 interacted with CAF1 in the presence of NOT1. **f** NOT3 interacted with CAF40 in the presence of NOT1. **g** NOT3 recruited CCR4 to the plasma membrane only in the presence of both NOT1 and CAF1. In the "Control" experiments the respective construct was coexpressed with the vector indicated at the top of the panel lacking an insert. The scale bar is 10 µm.

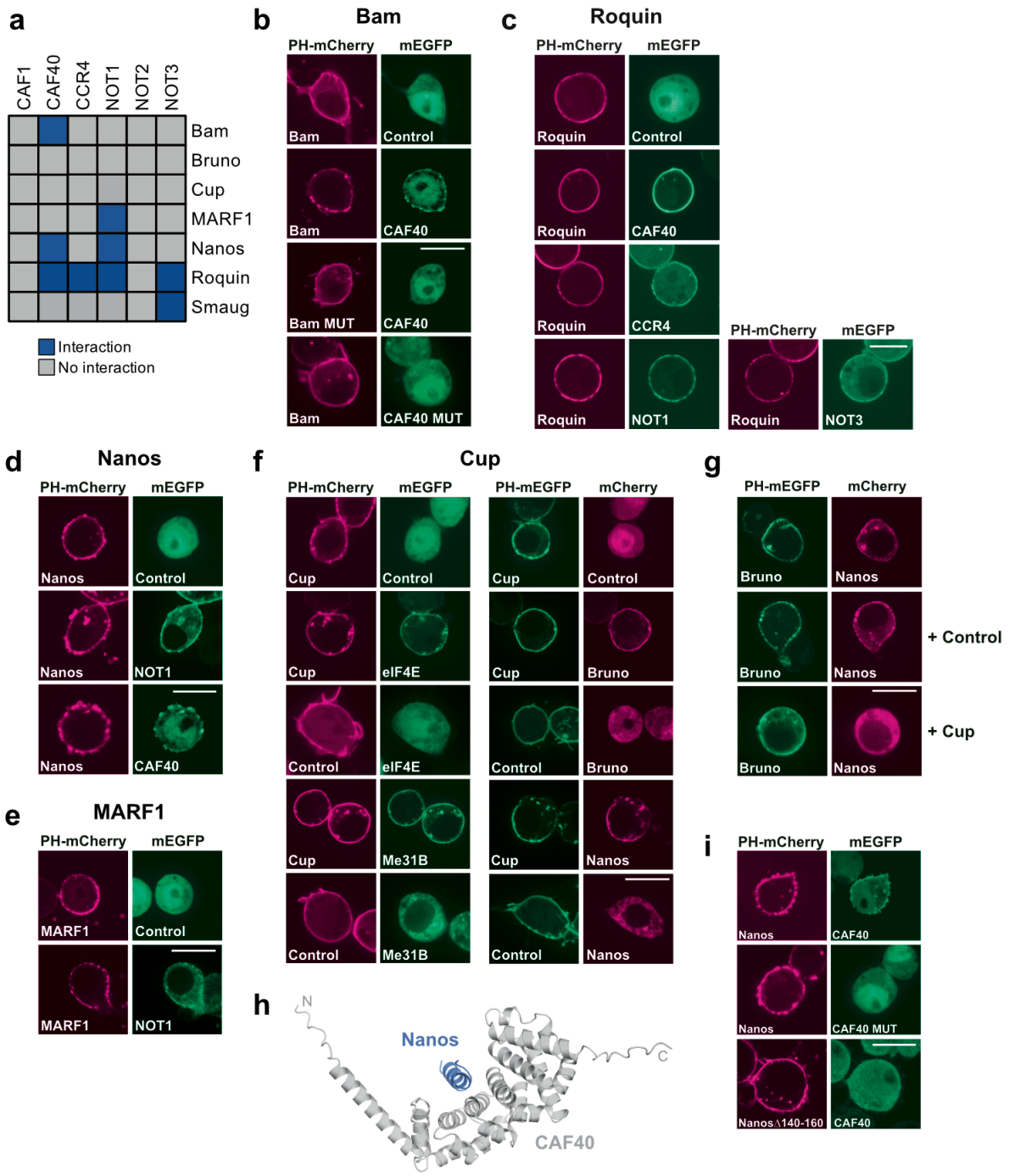

Fig. 4. PPIs between the CCR4-NOT complex and repressor proteins. Summary of the results (**a**) from a pairwise screen of CCR4-NOT complex core subunits with Bam (**b**), Nanos (**c**), Roquin (**d**), MARF1 (**e**), Bruno and Cup (**Supplementary Fig. 7**), and Smaug [63]. The blue color indicates an interaction, and the gray color indicates no interaction. Bam MUT carries the M24E and CAF40 MUT the V186E point mutation. **f** Cup interacted with eIF4E, Me31B, Bruno, and Nanos. **g** Bruno interacted with Nanos in the absence but not in the presence of Cup. In the "Control" experiments the respective construct was coexpressed with the vector indicated at the top of the panel lacking an insert. The scale bar is 10 µm.

576 **REFERENCES**
577

578 1. Masters, S. C. Co-immunoprecipitation from transfected cells. *Methods Mol*
579 *Biol* **261**, 337–350 (2004).
580 2. Ransone, L. J. Detection of protein-protein interactions by
581 coimmunoprecipitation and dimerization. *Methods Enzymol* **254**, 491–497
582 (1995).
583 3. Rigaut, G. *et al.* A generic protein purification method for protein complex
584 characterization and proteome exploration. *Nat Biotechnol* **17**, 1030–1032
585 (1999).
586 4. Gingras, A. C., Abe, K. T. & Raught, B. Getting to know the neighborhood:
587 using proximity-dependent biotinylation to characterize protein complexes and
588 map organelles. *Curr Opin Chem Biol* **48**, 44–54 (2019).
589 5. Bosch, J. A., Chen, C. L. & Perrimon, N. Proximity-dependent labeling methods
590 for proteomic profiling in living cells: An update. *Wiley Interdiscip Rev Dev Biol*
591 **10**, 1–17 (2021).
592 6. Roux, K. J. Marked by association: techniques for proximity-dependent labeling
593 of proteins in eukaryotic cells. *Cell Mol Life Sci* **70**, 3657–64 (2013).
594 7. Lalonde, S. *et al.* Molecular and cellular approaches for the detection of
595 protein-protein interactions: Latest techniques and current limitations. *Plant*
596 *Journal* **53**, 610–635 (2008).
597 8. Walport, L. J., Low, J. K. K., Matthews, J. M. & Mackay, J. P. The
598 characterization of protein interactions – what, how and how much? *Chem Soc*
599 *Rev* **50**, 12292–12307 (2021).
600 9. Remy, I. & Michnick, S. W. Application of protein-fragment complementation
601 assays in cell biology. *Biotechniques* **42**, 137–145 (2007).
602 10. Cui, Y. *et al.* Techniques for detecting protein-protein interactions in living cells:
603 principles, limitations, and recent progress. *Sci China Life Sci* **62**, 619–632
604 (2019).
605 11. Blaszczak, E., Lazarewicz, N., Sudevan, A., Wysocki, R. & Rabut, G. Protein-
606 fragment complementation assays for large-scale analysis of protein-protein
607 interactions. *Biochem Soc Trans* **49**, 1337–1348 (2021).
608 12. Wang, T. *et al.* Detecting Protein-Protein Interaction Based on Protein
609 Fragment Complementation Assay. *Curr Protein Pept Sci* **21**, 598–610 (2020).
610 13. Lv, S. *et al.* CAPPI: A Cytoskeleton-Based Localization Assay Reports Protein-
611 Protein Interaction in Living Cells by Fluorescence Microscopy. *Mol Plant* **10**,
612 1473–1476 (2017).
613 14. Grefen, C. *et al.* Subcellular localization and in vivo interactions of the
614 Arabidopsis thaliana ethylene receptor family members. *Mol Plant* **1**, 308–320
615 (2008).
616 15. Winkler, J. *et al.* Visualizing protein–protein interactions in plants by rapamycin-
617 dependent delocalization. *Plant Cell* **33**, 1101–1117 (2021).
618 16. Dixon, A. S. & Lim, C. S. The nuclear translocation assay for intracellular
619 protein-protein interactions and its application to the Bcr coiled-coil domain.
620 *Biotechniques* **49**, 519–524 (2010).
621 17. Lee, K. H., Lee, S., Lee, W. Y., Yang, H. W. & Heo, W. Do. Visualizing dynamic
622 interaction between calmodulin and calmodulin-related kinases via a
623 monitoring method in live mammalian cells. *Proc Natl Acad Sci U S A* **107**,
624 3412–3417 (2010).
625 18. Gallego, O. *et al.* Detection and Characterization of Protein Interactions In Vivo
626 by a Simple Live-Cell Imaging Method. *PLoS One* **8**, 1–6 (2013).

627 19. Taslimi, A. *et al.* An optimized optogenetic clustering tool for probing protein
628 interaction and function. *Nat Commun* **5**, 4925 (2014).
629 20. Martin, B. R., Deerinck, T. J., Ellisman, M. H., Taylor, S. S. & Tsien, R. Y.
630 Isoform-Specific PKA Dynamics Revealed by Dye-Triggered Aggregation and
631 DAKAP1α-Mediated Localization in Living Cells. *Chem Biol* **14**, 1031–1042
632 (2007).
633 21. Watanabe, T. *et al.* Genetic visualization of protein interactions harnessing
634 liquid phase transitions. *Sci Rep* **7**, 1–13 (2017).
635 22. Schneider, I. Cell lines derived from late embryonic stages of Drosophila
636 melanogaster. *J Embryol Exp Morphol* **27**, 353–365 (1972).
637 23. Yanagawa, S. I., Lee, J. S. & Ishimoto, A. Identification and characterization of
638 a novel line of Drosophila Schneider s2 cells that respond to wingless
639 signaling. *Journal of Biological Chemistry* **273**, 32353–32359 (1999).
640 24. Garcia, P. *et al.* The Pleckstrin Homology Domain of Phospholipase C-δ1
641 Binds with High Affinity to Phosphatidylinositol 4,5-Bisphosphate in Bilayer
642 Membranes. *Biochemistry* **34**, 16228–16234 (1995).
643 25. Lemmon, M. A., Ferguson, K. M., O'Brien, R., Sigler, P. B. & Schlessinger, J.
644 Specific and high-affinity binding of inositol phosphates to an isolated pleckstrin
645 homology domain. *Proc Natl Acad Sci U S A* **92**, 10472–10476 (1995).
646 26. Kim, H., Yan, Q., Von Heijne, G., Caputo, G. A. & Lennarz, W. J. Determination
647 of the membrane topology of Ost4p and its subunit interactions in the
648 oligosaccharyltransferase complex in Saccharomyces cerevisiae. *Proc Natl*
649 *Acad Sci U S A* **100**, 7460–7464 (2003).
650 27. Möckli, N. *et al.* Yeast split-ubiquitin-based cytosolic screening system to
651 detect interactions between transcriptionally active proteins. *Biotechniques* **42**,
652 725–730 (2007).
653 28. Jeske, M., Müller, C. W. & Ephrussi, A. The LOTUS domain is a conserved
654 DEAD-box RNA helicase regulator essential for the recruitment of Vasa to the
655 germ plasm and nuage. *Genes Dev* **31**, 939–952 (2017).
656 29. Breitwieser, W., Markussen, F. H., Horstmann, H. & Ephrussi, A. Oskar protein
657 interaction with vasa represents an essential step in polar granule assembly.
658 *Genes Dev* **10**, 2179–2188 (1996).
659 30. Jeske, M. *et al.* The crystal structure of the Drosophila germline inducer Oskar
660 identifies two domains with distinct Vasa Helicase- and RNA-binding activities.
661 *Cell Rep* **12**, 587–598 (2015).
662 31. Yang, N. *et al.* Structure of Drosophila Oskar reveals a novel RNA binding
663 protein. *Proc Natl Acad Sci U S A* **112**, 11541–11546 (2015).
664 32. Linder, P. & Jankowsky, E. From unwinding to clamping - the DEAD box RNA
665 helicase family. *Nat Rev Mol Cell Biol* **12**, 505–16 (2011).
666 33. Walker, J. E., Saraste, M., Runswick, M. J. & Gay, N. J. Distantly related
667 sequences in the alpha- and beta-subunits of ATP synthase, myosin, kinases
668 and other ATP-requiring enzymes and a common nucleotide binding fold.
669 *EMBO J* **1**, 945–951 (1982).
670 34. Gorbalenya, A. E., Koonin, E. V., Donchenko, A. P. & Blinov, V. M. A
671 conserved NTP-motif in putative helicases. *Nature* **333**, 22 (1988).
672 35. Xiol, J. *et al.* RNA clamping by Vasa assembles a piRNA amplifier complex on
673 transposon transcripts. *Cell* **157**, 1698–1711 (2014).
674 36. Stopa, N., Krebs, J. E. & Shechter, D. The PRMT5 arginine methyltransferase:
675 Many roles in development, cancer and beyond. *Cellular and Molecular Life*
676 *Sciences* **72**, 2041–2059 (2015).

677 37. Gonsalvez, G. B., Rajendra, T. K., Tian, L. & Matera, A. G. The Sm-Protein
678 Methyltransferase, Dart5, Is Essential for Germ-Cell Specification and
679 Maintenance. *Current Biology* **16**, 1077–1089 (2006).
680 38. Liu, H. *et al.* Structural basis for methylarginine-dependent recognition of
681 Aubergine by Tudor. *Genes Dev* **24**, 1876–1881 (2010).
682 39. Kirino, Y. *et al.* Arginine methylation of Aubergine mediates Tudor binding and
683 germ plasm localization. *RNA* **16**, 70–8 (2010).
684 40. Nishida, K. M. *et al.* Functional involvement of Tudor and dPRMT5 in the
685 piRNA processing pathway in Drosophila germlines. *EMBO Journal* **28**, 3820–
686 3831 (2009).
687 41. Kirino, Y. *et al.* Arginine methylation of Piwi proteins catalysed by dPRMT5 is
688 required for Ago3 and Aub stability. *Nat Cell Biol* **11**, 652–658 (2009).
689 42. Choi, J., Chen, J., Schreiber, S. L. & Clardy, J. Structure of the FKBP12-
690 rapamycin complex interacting with the binding domain of human FRAP.
691 *Science* **273**, 239–42 (1996).
692 43. Vassilev, L. T. *et al.* In Vivo Activation of the p53 Pathway by Small-Molecule
693 Antagonists of MDM2. *Science (1979)* **303**, 844–848 (2004).
694 44. Kussie, P. H. *et al.* Structure of the MDM2 oncoprotein bound to the p53 tumor
695 suppressor transactivation domain. *Science (1979)* **274**, 948–953 (1996).
696 45. Collart, M. A. & Panasenko, O. O. The Ccr4-Not Complex: Architecture and
697 Structural Insights. *Subcell Biochem* **83**, 349–379 (2017).
698 46. Temme, C., Simonelig, M. & Wahle, E. Deadenylation of mRNA by the CCR4-
699 NOT complex in Drosophila: molecular and developmental aspects. *Front*
700 *Genet* **5**, 143 (2014).
701 47. Brown, J. B. *et al.* Diversity and dynamics of the Drosophila transcriptome.
702 *Nature 2014 512:7515* **512**, 393–399 (2014).
703 48. Pizarro-Cerdá, J., Chorev, D. S., Geiger, B. & Cossart, P. The Diverse Family
704 of Arp2/3 Complexes. *Trends Cell Biol* **27**, 93–100 (2017).
705 49. Hu, Y., Comjean, A., Perrimon, N. & Mohr, S. E. The Drosophila Gene
706 Expression Tool (DGET) for expression analyses. *BMC Bioinformatics* **18**, 98
707 (2017).
708 50. Robinson, R. C. *et al.* Crystal Structure of Arp2/3 Complex. *Science (1979)*
709 **294**, 1679–1684 (2001).
710 51. Zhao, X., Yang, Z., Qian, M. & Zhu, X. Interactions among subunits of human
711 Arp2/3 complex: p20-Arc as the hub. *Biochem Biophys Res Commun* **280**,
712 513–517 (2001).
713 52. Stagljar, I., Korostensky, C., Johnsson, N. & Te Heesen, S. A genetic system
714 based on split-ubiquitin for the analysis of interactions between membrane
715 proteins in vivo. *Proc Natl Acad Sci U S A* **95**, 5187–5192 (1998).
716 53. Yang, J. & Reth, M. Drosophila S2 Schneider cells: a useful tool for rebuilding
717 and redesigning approaches in synthetic biology. *Methods Mol Biol* **813**, 331–
718 41 (2012).
719 54. Sgromo, A. *et al.* Drosophila Bag-of-marbles directly interacts with the CAF40
720 subunit of the CCR4-NOT complex to elicit repression of mRNA targets. *RNA*
721 **24**, 381–395 (2018).
722 55. Sgromo, A. *et al.* A CAF40-binding motif facilitates recruitment of the CCR4-
723 NOT complex to mRNAs targeted by Drosophila Roquin. *Nat Commun* **8**,
724 14307 (2017).
725 56. Raisch, T. *et al.* Distinct modes of recruitment of the CCR4-NOT complex by
726 Drosophila and vertebrate Nanos. *EMBO J* **35**, 974–90 (2016).

57. Zhu, L., Kandasamy, S. K., Liao, S. E. & Fukunaga, R. LOTUS domain protein MARF1 binds CCR4-NOT deadenylase complex to post-transcriptionally regulate gene expression in oocytes. *Nat Commun* **9**, 4031 (2018).
58. Semotok, J. L. *et al.* Smaug recruits the CCR4/POP2/NOT deadenylase complex to trigger maternal transcript localization in the early Drosophila embryo. *Curr Biol* **15**, 284–94 (2005).
59. Zaessinger, S., Busseau, I. & Simonelig, M. Oskar allows nanos mRNA translation in Drosophila embryos by preventing its deadnylation by Smaug/CCR4. *Development* **133**, 4573–4583 (2006).
60. Smibert, C. A., Wilson, J. E., Kerr, K. & Macdonald, P. M. smaug protein represses translation of unlocalized nanos mRNA in the Drosophila embryo. *Genes Dev* **10**, 2600–9 (1996).
61. Dahanukar, A. & Wharton, R. P. The Nanos gradient in Drosophila embryos is generated by translational regulation. *Genes Dev* **10**, 2610–2620 (1996).
62. Dahanukar, A., Walker, J. A. & Wharton, R. P. Smaug, a novel RNA-binding protein that operates a translational switch in Drosophila. *Mol Cell* **4**, 209–218 (1999).
63. Pekovic, F. *et al.* RNA binding proteins Smaug and Cup induce CCR4–NOT-dependent deadenylation of the *nanos* mRNA in a reconstituted system. *Nucleic Acids Res* **51**, 3950–3970 (2023).
64. Nelson, M. R., Leidal, A. M. & Smibert, C. A. Drosophila Cup is an eIF4E-binding protein that functions in Smaug-mediated translational repression. *EMBO J* **23**, 150–9 (2004).
65. Nakamura, A., Sato, K. & Hanyu-Nakamura, K. Drosophila Cup is an eIF4E binding protein that associates with Bruno and regulates oskar mRNA Translation in Oogenesis. *Dev Cell* **6**, 69–78 (2004).
66. Wilhelm, J. E., Hilton, M., Amos, Q. & Henzel, W. J. Cup is an eIF4E binding protein required for both the translational repression of oskar and the recruitment of Barentsz. *Journal of Cell Biology* **163**, 1197–1204 (2003).
67. Zappavigna, V., Piccioni, F., Villaescusa, J. C. & Verrott, A. C. Cup is a nucleocytoplasmic shuttling protein that interacts with the eukaryotic translation initiation factor 4E to modulate Drosophila ovary development. *Proc Natl Acad Sci U S A* **101**, 14800–14805 (2004).
68. Kamenska, A. *et al.* The DDX6-4E-T interaction mediates translational repression and P-body assembly. *Nucleic Acids Res* **44**, 6318–6334 (2016).
69. Ozgur, S. *et al.* Structure of a Human 4E-T/DDX6/CNOT1 Complex Reveals the Different Interplay of DDX6-Binding Proteins with the CCR4-NOT Complex. *Cell Rep* **13**, 703–711 (2015).
70. Kinkelin, K., Veith, K., Grünwald, M. & Bono, F. Crystal structure of a minimal eIF4E-Cup complex reveals a general mechanism of eIF4E regulation in translational repression. *Rna* **18**, 1624–1634 (2012).
71. Igreja, C. & Izaurralde, E. CUP promotes deadenylation and inhibits decapping of mRNA targets. *Genes Dev* **25**, 1955–1967 (2011).
72. Verrotti, A. C. & Wharton, R. P. Nanos interacts with Cup in the female germline of Drosophila. *Development* **127**, 5225–5232 (2000).
73. Kim, G. *et al.* Region-Specific Activation of oskar mRNA Translation by Inhibition of Bruno-Mediated Repression. *PLoS Genet* **11**, 1–22 (2015).
74. Bansal, P., Madlung, J., Schaaf, K., Macek, B. & Bono, F. An Interaction Network of RNA-Binding Proteins Involved in Drosophila Oogenesis. *Molecular and Cellular Proteomics* **19**, 1485–1502 (2020).

75. Evans, R. *et al.* Protein complex prediction with AlphaFold-Multimer. *bioRxiv* 2021.10.04.463034 (2021) doi:https://doi.org/10.1101/2021.10.04.463034.
76. Jumper, J. *et al.* Highly accurate protein structure prediction with AlphaFold. *Nature* **596**, 583–589 (2021).
77. Mirdita, M. *et al.* ColabFold: making protein folding accessible to all. *Nature Methods 2022 19:6* **19**, 679–682 (2022).
78. Ivanov, A. A., Khuri, F. R. & Fu, H. Targeting protein-protein interactions as an anticancer strategy. *Trends Pharmacol Sci* **34**, 393–400 (2013).
79. Buchwald, P. Small-molecule protein-protein interaction inhibitors: Therapeutic potential in light of molecular size, chemical space, and ligand binding efficiency considerations. *IUBMB Life* **62**, 724–731 (2010).
80. Behm-Ansmant, I. *et al.* mRNA degradation by miRNAs and GW182 requires both CCR4:NOT deadenylase and DCP1:DCP2 decapping complexes. *Genes Dev* **20**, 1885–98 (2006).
81. Vonkova, I. *et al.* Lipid Cooperativity as a General Membrane-Recruitment Principle for PH Domains. *Cell Rep* **12**, 1519–30 (2015).
82. Schindelin, J. *et al.* Fiji: An open-source platform for biological-image analysis. *Nat Methods* **9**, 676–682 (2012).